ISSN: 2997-6170

Research Article

Space Science Journal

Model Based Maximum Likelihood Detector for Optical Communications Systems Employing the Nonlinear Fourier Transform

Ofer Aluf*

School of Electrical & Computer Engineering, Ben Gurion University of the Negev, Beer Sheva 84105, Israel

***Corresponding Author**
Ofer Aluf, School of Electrical & Computer Engineering, Ben Gurion University of the Negev, Beer Sheva 84105, Israel.

Submitted: 2026, Mar 09; **Accepted**: 2026, Apr 06; **Published**: 2026, Apr 10

Citation: Aluf, O. (2026). Model Based Maximum Likelihood Detector for Optical Communications Systems Employing the Nonlinear Fourier Transform. *Space Sci J, 3*(2), 01-06

Abstract

Optical communication systems are implemented in many systems and employ the nonlinear fourier transform (NFT). The use of the model is based on a maximum likelihood detector. The fiber communication system is described by the NFT scheme and by Digital Signal Processing (DSP) architecture. We use the previously developed analytical model for the nonlinear frequency division multiplexing channel to develop a maximum likelihood detection scheme for both symbol-wise detection and (if possible) sequence detection via the Viterbi algorithm with quantized observed samples.

Keywords: Maximum Likelihood (ML), Optical Communication, Nonlinear Fouriertransform (NFT), Digital Signal Processing (DSP), Symbol-Wise Detection, NPDE, NFDM, Zakharov-Shabat Eigenvalue, INFT, Symbol Mapping, Scaling, Pre-Compensation, Gb Insertion, Coherent Detection, Post-Compensation, ML Symbol Detection, Gaussian Noise, Delta-Correlated Gaussian Noise, B-Coefficient, Clipped Linear Mapping, Covariance, Pseudocovariance, RRC, ML Sequence Detection, WDM, MLD, Quantum Noise, Spatial Division Multiplexing (SDM), NLSE, Nonlinear Schrodinger Equation (NLSE)

1. Introduction

The Nonlinear Fourier Transform (NFT) is widely used in many scientific and industrial applications. It is a good mathematical technique to obtain the solution of nonlinear partial differential equations (NPDEs). One type of nonlinear partial differential equation is Nonlinear Schrodinger equation (NSE). The way NFT technique uses to solve NPDEs is by decomposing complex signals into nonlinear spectrum components. The nonlinear spectrum components are described as discrete eigenvalues and reflection coefficients. We use NFT techniques in fiber optics (FOs) to analyze non-dispersive solitons and nonlinear radiation. It is done directly by addressing nonlinearity with no previous methods to compensate. The capacity in fiber optics (FOs) is a very critical issue since the demands are increasing all the time. The fiber optics nonlinear effects influence the FOs spectral efficiency by limiting it. Nonlinearity compensation is the way to compensate for it and get high fiber optics capacity. Fiber optics suffer from nonlinearity due to the Kerr effect. In this paper, we first discuss the Zakharov - Shabat eigenvalue problem and then characterize the Nonlinear Frequency Division Multiplexing (NFDM) communication scheme. It is a standard scaled modulation scheme b for NFDM. The channel model includes the input and output model and the fiber optic channel law. The symbol wise Maximum Likelihood (ML) detection method is discussed for best performance. The best performances are achieved by using symbol-wise detection. Performances are improved by controlling the error rates (SER/BER) and signal constellation architecture. The Digital Signal Processing (DSP) in the transmitter and receiver communication system internal functional blocks are described.

2. System setup

2.1. Zakharov-Shabat Eigenvalue Problem

The forward NFT is computed via the so-called Zakharov-Shabat eigenvalue problem [1-3] for a thorough exposition to the subject. Briefly, the direct NFT is computed from specific solutions of the systems of equations [1]:

$$\frac{d\phi_1}{dt} = q(t)\,\phi_2 - i\zeta\phi_1\,, \qquad \frac{d\phi_2}{dt} = -\bar{q}(t)\,\phi_1 + i\zeta\phi_2 \tag{1}$$

for different values of the complex spectral parameter ζ. The overbar in (1) and Below stands for the complex conjugate [1–3]. Eqs.(1) are solved with the boundary conditions: $(\phi_1(t), \phi_2(t))^T \to (e^{-i\zeta t}, 0)^T$ when $t \to -\infty$.

2.2. NFDM Communication Scheme

Here we shall use a standard scaled b-modulation scheme for NFDM previously used in multiple studies [4–7]. The basics of the scheme are shown in Figure 1. At the transmitter, the bit sequences are mapped into a symbol sequence, each having m-bits which are mapped into the initial *loading spectrum* consisting of N_{sc} orthogonal subcarriers, ψ_n :

$$u_{in}(\xi) = \sqrt{S} \sum_{n=0}^{N_{sc}-1} c_n \psi_n(\xi) \tag{2}$$

where S is the dimensionless power scaling factor. Next, due to the natural amplitude limitation of the b-coefficient, $0 \le |b(\xi)| \le 1$ and amplitude squeezing is applied:

$$b_{in}(\xi) = f(|u_{in}(\xi)|)\, e^{i\angle u_{in}(\xi)} \tag{3}$$

where $0 \le f\ (x) \le 1$ is a monotonically increasing function for which the mapping is invertable. Later we shall discuss possible choices of the squeezing function. The half-way precompensation is used to increase spectral efficiency: $b(0, \xi) = b_{in}(\xi) \exp(-i\, \xi^2_L)$ where L is the propagation distance in dimensionless units. This is the initial nonlinear spectrum after the INFT operation, is launched in the fiber. At the receiver, after coherent detection, the above operations are reversed and one ends up with the output loading spectrum $u_{out}\ (\xi)$. This spectrum is generally corrupted by a few types of noise (see below). Using the orthogonality of the carriers, the output complex symbols are estimated.

$$\hat{c}_n = S^{-1/2} \int u_{out}(\xi)\, \psi_n^*(\xi)\, d\xi, \quad n = 0, \ldots, N_{sc} - 1 \tag{4}$$

Digital Signal Processing (DSP) is related to Nonlinear Fourier Transform (NFT) based communication system. It can also be mentioned on Nonlinear Frequency Division Multiplexing (NFDM) for managing the fiber optic nonlinearity. It is done by encoding the information in the nonlinear spectrum rather than the linear frequency domain. We have two communication sides, DSP communication system. The first side is the DSP transmitter (Tx) and the other side is the DSP receiver (Rx). The function of DSP transmitter is to mapping data spectral components and create the related time domain signal. The information data are mapped onto the nonlinear spectrum. Then scaling and pre compensation. Signal shaping is done by Nyquist Root Raised Cosine (RRC) filtering. Pre-compensation is done by pre-distortion, and it compensates for the transmitter hardware limitations. Then the signal converts the nonlinear spectrum to a time domain complex envelope signal by Invers NFT (INFT). Finnaly, GB insertion

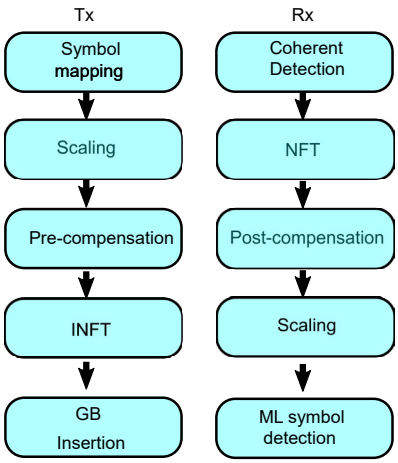

Figure 1: Digital Signal Processing (Dsp) at the Transmitter and the Receiver Communication System Architecture

is done before transmitting the data through the fiber optic channel. The DSP receiver function is to retrieve information from the received time domain signal. Data retrieving is important, since it is distorted by noise and fiber optic nonlinearity effects. We have communication system opposite functionality blocks at the DSP receiver. The functionality blocks are coherent detection, NFT conversion, data post compensation, data scaling, and ML symbol detection.

3. Results

3.1. The Input Output Model and the Channel Law

The channel model for the b-modulated NFDM transmission was developed in. It reads:

$$b_{out}(\xi) = b_{in}(\xi) + (1-|b_{in}(\xi)|^2)^{1/2}\, N(\xi) + N_p(\xi), \qquad \mathrm{E}\left[N(\xi)\bar{N}(\xi')\right] = n_{ASE}\,\delta(\xi-\xi') \quad (5)$$

where $N(\xi)$ is the circular symmetric delta-correlated Gaussian noise and the last term in the r.h.s describes the processing noise [8]. The latter is important at high values of the input power, and since no analytical model exists for it, we shall not be able to compensate for it.

3.2. ML Symbol-Wise Detection

To enable symbol-wise detection, we need to linearize the input-output relation w.r.t. ASE noise. The result is [6]:

$$\begin{aligned} u_{out}(\xi) &= u_{in}(\xi) + g_+(|u_{in}(\xi)|)\, N(\xi) + g_-(|u_{in}(\xi)|)\, e^{2i\,\angle u_{in}(\xi)}\, N^*(\xi) \\ g_\pm(x) &= \frac{\sqrt{1-f^2(x)}}{2}\left(\frac{1}{f'(x)} \pm \frac{x}{f(x)}\right) \end{aligned} \quad (6)$$

The received symbols are estimated via Eq.(4) leading to zero-mean correlated Gaussian model:

$$\begin{aligned} \hat{c}_n &= c_n + N_n \\ N_n &= \frac{1}{\sqrt{S}}\left[\int g_+(|u_{in}(\xi)|)\,\psi_n^*(\xi)\,N(\xi)d\xi + \int g_-(|u_{in}(\xi)|)\,e^{2i\,\angle u_{in}(\xi)}\,\psi_n^*(\xi)\,N^*(\xi)d\xi\right] \\ \mathbb{E}[N_n\,N_{n'}^*] &= \frac{n_{ASE}}{S}\int \psi_n^*(\xi)\,\left[g_+^2(|u_{in}(\xi)|) + g_-^2(|u_{in}(\xi)|)\right]\,\psi_{n'}(\xi)\,d\xi \\ \mathbb{E}[N_n\,N_{n'}] &= \frac{2\,n_{ASE}}{S}\int \psi_n^*(\xi)\,g_+(|u_{in}(\xi)|)\,g_-(|u_{in}(\xi)|)\,e^{2i\,\angle u_{in}(\xi)}\,\psi_{n'}^*(\xi)\,d\xi \end{aligned} \quad (7)$$

Note that both covariance and pseudocovariance matrices above depend on the whole sequence via the absolute value of the input loading spectrum $u_{in}(\xi)$.

3.2.1. The Choice of the Scaling Function

Let us now discuss the choice of the scaling function $u \to b\,f\,(x)$ - Eq.(3). So far, the only function used in the literature was exponential squeeze mapping for which:

$$\begin{aligned} f(x) &= \left[1-\exp(-x^2)\right]^{1/2} \\ g_\pm(x) &= \frac{1}{2x\,\sqrt{\exp(x^2)-1}}\left(\exp(x^2) - 1 \pm x^2\right) \end{aligned} \quad (8)$$

Note, however, that at large values of the argument both $g\pm$ are growing exponentially, and hence the noise variance and covariances according to (7). There is no contradiction with the theoretical noise squeeze result (5) since this limits the linearization procedure used to obtain the connection between the input and output loading spectrum is no longer applicable. This was already noted in since at large values of the power of the loading spectrum u the exponential squeezing function (8) is strongly saturated, so even small changes of the b-coefficient due to noise (5) translate into large variations of the loading spectrum which contains the modulated symbol. Therefore, the linearized model (6) is strictly valid only for the arguments $|u_{in}| \sim 1$ or smaller. This prompts us to search for an alternative scaling for the b-coefficient. We suggest a *clipped linear* mapping defined as:

$$f(x) = \begin{cases} \alpha\, x & x \le x_{max} = (1-\varepsilon)/\alpha \\ 1-\varepsilon & x \ge x_{max} \end{cases} \quad (9)$$

In other words, the relation is linear up to the maximum allowed amplitude of the loading spectrum, $x_{max} = |u(\xi)|_{max}$ and is cut to this value for larger amplitudes. The reason why we use $1-\varepsilon$ as opposed to the maximum theoretical value of 1 for the clipping threshold is that most numerical NFT routines fail when the b-coefficient approaches this barrier (since this case corresponds to the infinite r coefficient and the infinite burst power) [9]. Therefore, we use a small offset $\varepsilon \ll 1$ where one can still rely on the numerical accuracy of the NFT routines. The first benefit of using this scaling is that since below the threshold the model (6), (7) becomes *exact* (in the same regime as (5) is valid) if one assumes:

$$g_+(x) = \begin{cases} \frac{\sqrt{1-(\alpha x)^2}}{\alpha} & x \le x_{max} \\ (1-(1-\varepsilon)^2)^{1/2} \approx \sqrt{2\varepsilon} & x > x_{max} \end{cases} \qquad (10)$$
$$g_-(x) = 0$$

Note how the pseudocovariance vanishes in this approach and the noise becomes indeed squeezed as x approaches x_{max}. The caveat of this scaling is, of course, that in the spectral regions where the amplitude is above threshold, the clipping introduces additional errors even without ASE noise. This can become especially pronounced for dense overlapping formats like HG. Therefore, care must be taken when selecting the amplitude cutoff x_{max}. Of course, the clipping error can be completely avoided (at least in the deterministic case) by choosing $x_{max} = \max_{\xi} |u_{in}(\xi)|$. However, this quantity is, however, strongly sequence dependent and is not known at the transmitter. Therefore, the alternative is to calculate the average value of the amplitude of the loading spectrum $|u_{in}(\xi)|$ where the averaging is performed on the input sequences (2). This average is not available analytically, but one can simplify the calculation noticing that the symbols c_n are i.i.d. and in the limit of the large number of subcarriers $N_{sc} \gg 1$ the loading spectrum at each point can be approximated by a zero mean Gaussian process (as no power bias is assumed for the constellation). Then $|u_{in}(\xi)|$ is a Rayleigh distributed with the mean given by $\overline{|u_{in}(\xi)|} = (|u_{in}(\xi)|^2\,\pi/4)^{1/2}$. The averaged second moments for sincs and HGs are given by [6,8,10]:

$$\overline{|u_{in}(\xi)|^2} = \begin{cases} S\,\sigma^2\,\frac{\sqrt{2N_{sc}}}{\pi} & \text{HG} \\ S\,\sigma^2 & \text{Sincs} \end{cases} \qquad (11)$$

where the average is taken over an independent and Identically Distributed (i.i.d) constellation symbols with zero mean and variance $|c_n|^2 = \sigma^2$ and over the nonlinear spectral bandwidth. This gives a typical scale to be used for the clipping amplitude x_{max}.

3.2.2. Simplified Covariance and Pseudocovariance Matrices

For symbol-wise detection one must only consider the diagonal elements of the covariance and pseudo-covariance matrices (7) when $n = n'$. The resulting expressions can be simplified when the nonlinear subcarriers are either non-overlapping (as in finite support carriers of) or weakly overlapping like e.g. RRC. In this case, one can follow the approach of Ref. and notice that only the current subcarrier contributes to the spectral integrals (7) so that one can approximate $|u_{in}(\xi)| \approx S\,c_n\,\psi_n(\xi)$ when evaluating the variance and pseudovariance of the sent symbol c_n. Thus, the channel becomes not only conditionally Gaussian but ISI-free with the variance and pseudovariance depending only on the sent symbol and the squeezing function:

$$\mathbb{E}[N_n\,N_n^*] = \sigma^2(c_n) = \frac{n_{ASE}}{S}\int |\psi_n(\xi)|^2\left[g_+^2(\sqrt{S}|c_n\,\psi_n(\xi)|) + g_-^2(\sqrt{S}|c_n\,\psi_m(\xi)|)\right]d\xi$$
$$\mathbb{E}[N_n\,N_n] = \tilde{\sigma}^2(c_n) = \frac{2\,n_{ASE}}{S}\int (\psi_n^*(\xi))^2\,g_+(\sqrt{S}|c_n\,\psi_n(\xi)|)\,g_-(\sqrt{S}|c_n\,\psi_n(\xi)|)\,e^{2i\sqrt{S}\angle(c_n\,\psi_n(\xi))}\,d\xi \qquad (12)$$

For the case of exponential mapping, the integrals involved are not available analytically and should be evaluated numerically. However, for the clipped linear mapping, the situation simplifies significantly. In this case the pseudo-variance vanishes and for the variance one obtains

$$\sigma^2(c_n) = \frac{n_{ASE}}{S}\left[\int_{|u_{in}(\xi)|<x_{max}} |\psi_n(\xi)^2|\,(\alpha^{-2} - |u_{in}(\xi)|^2)\,d\xi + \sqrt{2\varepsilon}\int_{|u_{in}(\xi)|>x_{max}} d\xi\right] \qquad (13)$$

Note that since $|u_{in}|^2 < x_{max}^2 = (1-\varepsilon)^2/\alpha^2$ the first integral is always positive. In order to proceed, we shall make a few assumptions. First, we neglect the second integral which is justified for $\varepsilon \ll 1$ and enlarge the integration of the first integral to the whole nonlinear spectrum domain. This is justified for large thresholds x_{max} when spectral outages are rare and their contribution to the integral is neglected. Note that it may happen that the integral defined above can become negative in rare cases at large values of input power S - in which case we shall simply clip it from below by zero (or rather a small machine threshold, δ). Next we shall specify the specific form of the carriers, i.e. sinc pulses (RRC carriers with the vanishing roll-off factor) for which the integral can be evaluated exactly leading to:

$$\sigma^2(c_n) = \frac{n_{ASE}}{S}\left[\alpha^{-2} - S\sum_{i,j=0}^{N_{sc}-1} I_{nij}\, c_i\, c_j^*\right]_+$$

$$I_{nij} = \int |\psi_n(\xi)|^2\, \psi_i(\xi)\, \psi_j(\xi)\, d\xi = \begin{cases} \frac{(-1)^{i-j}}{2\pi^2 (i-n)(j-n)}, & i \neq j \neq n \\ \frac{1}{\pi^2 (i-n)^2}, & i = j \neq n \\ \frac{2}{3}, & i = j = n \end{cases} \qquad (14)$$

where, $[\,.\,.\,.]^+$ is denoted rectify linear operation suppresses negative argument and leaves positive one unchanged (in practice, one should use a small machine-precision threshold δ or a soft rectifier function).

Note that due to the assumptions made during its derivation of Eq.(14) under estimates the noise variance. One can also see that the main contribution to the variance comes from the diagonal term I_{nnn} so that in the main approximation one gets memoryless channel model with the variance:

$$\sigma^2(c_n) = \frac{n_{ASE}}{S}\left[\alpha^{-2} - \frac{2S}{3}|c_n|^2\right]_+ \qquad (15)$$

This simplified model does capture the noise squeezing effect in the channel model for b coefficient higher energy constellation points have reduced noise variance.

3.3. ML Sequence Detection

The symbol-wise detection considered previously did not take into account correlations between different symbols and hence is suboptimal. For weakly overlapping symbols, one can approximate the covariance and pseudocovariance matrices as approximately diagonal, which signifies weak correlation between the noise for different symbols. Since the noise statistics conditioned on the input is Gaussian in our model, this signifies conditional independence of the symbols, so that sequence detection should amounts to the symbol-wise detection as considered in the previous subsection

4. Discussion

In optical communication the maximum achievable capacity is inspecting for getting the maximum data rate a fiber optic channel can transmit. We can get data rate which exceed 100 Tbps/fiber if we use wavelength division multiplexing (WDM) and coherent data technologies. If we use C and L bands then capacity maximization is achievable. It utilizes spatial division multiplexing (SDM) with multi-core fiber optics. The laser transmitter is an element of binary optical communication system and includes a likelihood ratio decision box. The optical communications and achieving optical performance are related the handshake between channel capacity and maximum likelihood detector (MLD). Quantum noise and atmospheric interferences limit the optical channel performances. We want to transmit data through fiber optic channel with maximum data rate and minimal errors. The fiber optic channel capacity is limited by fiber nonlinearity (Kerr nonlinearity effect) and noises. The fiber nonlinearity increases when the data signal strength increases and create phenomenon of "capacity ceiling". There are few capacity enhancing technologies in use. The maximum likelihood detector (MLD) minimized the probability of errors by choosing the "most likely" transmitted signal which yield the actual received signal. The MLD detector performs a statistical calculation which is based on channel noise model and choose a value that satisfied $m = \arg\max P(c/m)$, when c is the received signal and m is the signal that is sent. The nonlinear Fourier transform (NFT) is optical fiber advance signal processing technique that take care fiber nonlinearity as a source rather than a channel limitation. The channel signals are transformed into nonlinear spectral data and decouples the nonlinear Schrodinger equation (NLSE). By that we get managed Kerr nonlinearity which increase the spectral efficiency. NFDM method uses NFT to encode information data onto nonlinear spectral components. They are evolve linearity in the transform domain. The "eigenvalue communication" is NFT based communication and help to get the physical reality optical fibers [10-12].

References

1. Shabat, A., & Zakharov, V. (1972). Exact theory of two-dimensional self-focusing and one-dimensional self-modulation of waves in nonlinear media. *Sov. Phys. JETP, 34*(1), 62.

2. M. Yousefi and F. Kschischang, "Information transmission using the nonlinear Fourier transform, Part I–III," IEEE Trans. Inf. Theory **60**, 4312 (2014).
3. Turitsyn, S. K., Prilepsky, J. E., Le, S. T., Wahls, S., Frumin, L. L., Kamalian, M., & Derevyanko, S. A. (2017). Nonlinear Fourier transform for optical data processing and transmission: advances and perspectives. *Optica, 4*(3), 307-322.
4. Yangzhang, X., Aref, V., Le, S. T., Buelow, H., Lavery, D., & Bayvel, P. (2019). Dual-Polarization Non-Linear Frequency-Division Multiplexed Transmission With-Modulation. *Journal of Lightwave Technology, 37*(6), 1570-1578.
5. X. Yangzhang, V. Aref, S. T. Le, H. Buelow, D. Lavery, and P. Bayvel, "Experimental Demonstration of Dualpolarisation NFDM Transmission with b-Modulation," IEEE Photonics Technology Letters **31**(11), 885–888 (2019).
6. Derevyanko, S., Balogun, M., Aluf, O., Shepelsky, D., & Prilepsky, J. E. (2021). Channel model and the achievable information rates of the optical nonlinear frequency division-multiplexed systems employing continuous b-modulation. *Optics Express, 29*(5), 6384-6406.
7. Balogun, M., & Derevyanko, S. (2021). Hermite-Gaussian nonlinear spectral carriers for optical communication systems employing the nonlinear Fourier transform. *IEEE Communications Letters, 26*(1), 109-112.
8. Pankratova, M., Vasylchenkova, A., Derevyanko, S. A., Chichkov, N. B., & Prilepsky, J. E. (2020). Signal-noise interaction in optical-fiber communication systems employing nonlinear frequency-division multiplexing. *Physical Review Applied, 13*(5), 054021.
9. Wahls, S., Chimmalgi, S., & Prins, P. J. (2018). FNFT: A software library for computing nonlinear Fourier transforms. *Journal of Open Source Software, 3*(23), 597.
10. Balogun, M., & Derevyanko, S. (2022). Enhancing the spectral efficiency of nonlinear frequency division multiplexing systems via Hermite-Gaussian subcarriers. *Journal of Lightwave Technology, 40*(18), 6071-6077.
11. Wahls, S. (2017, February). Second order statistics of the scattering vector defining the dt nonlinear fourier transform. In *SCC 2017; 11th International ITG Conference on Systems, Communications and Coding* (pp. 1-6). VDE.
12. Gui, T., Zhou, G., Lu, C., Lau, A. P. T., & Wahls, S. (2018). Nonlinear frequency division multiplexing with b-modulation: shifting the energy barrier. *Optics express, 26*(21), 27978-27990.